Available online at www.sciencedirect.com
ScienceDirect
Journal of Solid State Chemistry 180 (2007) 1141–1148
JOURNAL OF SOLID STATE CHEMISTRY
www.elsevier.com/locate/jssc

A new molecular precursor route for the synthesis of Bi–Y, Y–Nb and Bi-doped Y–Nb oxides at moderate temperatures

D.A. Bayot, A.M. Dupont, Michel M. Devillers*

Unité de Chimie des Matériaux Inorganiques et Organiques, Université Catholique de Louvain, Place Louis Pasteur 1, B-1348 Louvain-la-Neuve, Belgium

Received 4 December 2006; received in revised form 25 January 2007; accepted 28 January 2007
Available online 8 February 2007

Abstract

Yttrium-based multimetallic oxides containing bismuth and/or niobium were prepared by a method starting from pre-isolated stable water-soluble precursors which are complexes with the ethylenediaminetetraacetate ligand (edta). The cubic $Bi_{1-x}Y_xO_{1.5}$ ($x = 0.22$, 0.25 and 0.3) and Y_3NbO_7 oxides were obtained in a pure form in a range of moderate temperatures (600–650 °C). This preparation method also allowed to stabilize at room temperature, without quenching, the tetragonal $YNbO_4$ oxide in a distorted form (T′-phase) by calcining the precursor at 800 °C. When heated up to 1000 °C, this metastable T′-phase transforms into the metastable "high-temperature" T oxide, which converts on cooling down to room temperature into the thermodynamically stable monoclinic M oxide. Doping the $YNbO_4$ oxide with Bi^{3+} cations (0.5% and 1% Bi with respect to total Bi + Y amount) led at 800 °C to a mixture of the T′-phase and the thermodynamically stable monoclinic one. At 900 °C, the almost pure monoclinic structure was obtained.

Keywords: Yttrium; Niobium; Bismuth; Oxides; Precursors

1. Introduction

Yttrium-containing multimetallic oxides generate considerable interest in many challenging fields. They have been under constant investigation over the last few years because of their attractive properties in two main domains of applications, namely ionic conductivity and luminescence. Such Y-based materials are, for example, really promising as solid electrolytes for solid oxide fuel cells (SOFCs) or electrochemical sensors, and as phosphors, display monitors, X-ray imaging or amplifiers for fiber-optic communications, respectively. It is now well established that the formulations and crystalline structures of the yttrium-based oxides aimed for each of the two applications are radically different.

In the case of ionic conductivity, the yttrium-based oxides investigated up to now are derived from the defect fluorite-like δ-Bi_2O_3 phase, which displays excellent properties in this context (its conductivity at 800 °C reaches 2.3 S cm^{-1}) [1]. Unfortunately, this well-known cubic oxide is stable between 730 and 825 °C only [2]. However, it is known that it can be stabilized at room temperature by partially substituting Bi^{3+} ions by other cations such as lanthanides(III) or yttrium(III), while preserving the fluorite-type structure and keeping appreciable values of ionic conductivity [3–5]. Particularly, when doping Bi_2O_3 by Y_2O_3, a solid solution of general formula $(Bi_2O_3)_{1-x}(Y_2O_3)_x$, also noted $Bi_{1-x}Y_xO_{1.5}$, is formed and it can adopt a rhombohedral or a cubic lattice [6–9]. When the cubic lattice is reached, the material shows the higher values of conductivity in the range of x between 0.2 and 0.3 (when $x = 0.25$, the conductivity at 600 °C is $4.38.10^2$ S cm^{-1}) [1]. Moreover, next to these Bi_2O_3-derived phases, yttrium-based oxides containing niobium(V) have also recently been studied in the same context. A fluorite-structured solid solution, which corresponds to the general formula $Y_{1-x}Nb_xO_{1.5+x}$, but which is often written as Y_3NbO_7 (when $x = 0.25$), has been reported in the Y_2O_3–Nb_2O_5 system [10–15] and displays a significantly

*Corresponding author. Fax: +32 10 472330.
E-mail address: devillers@chim.ucl.ac.be (M.M. Devillers).

0022-4596/$ - see front matter © 2007 Elsevier Inc. All rights reserved.
doi:10.1016/j.jssc.2007.01.027

high ionic conductivity due to its oxygen vacancies [11,12,14,15]. In another context, yttrium-based multimetallic oxides are famous for their luminescent properties, and previous studies dealt essentially with vanadate [16,17], niobate [18–20] and tantalate [20–23] materials. These oxides, which correspond to the YVO_4, $YNbO_4$ and $YTaO_4$ stoichiometries, respectively, are actually known to luminesce under UV and/or X-ray excitation, but they are often doped with tervalent cations such rare-earth ions (Ce^{3+}, Pr^{3+}, Eu^{3+}, etc.) [24,25] and often Bi^{3+} [19,26,27] to improve the luminescence efficiency.

The purpose of this work is to develop new synthetic routes to these particular oxides, namely the $Bi_{1-x}Y_xO_{1.5}$ solid solution, the Y_3NbO_7 phase and undoped and Bi-doped $YNbO_4$ oxides. The usual way to prepare these materials so far is based on solid-state reactions between the binary oxides involved, i.e., Y_2O_3, Bi_2O_3 and/or Nb_2O_5. This so-called ''ceramic method'' requires heat treatments at very high temperatures reaching sometimes 1500 °C, as well as repeated grinding procedures in order to obtain the desired mixed oxide. Moreover, this way commonly results in unpure oxides, like, for example, in the case of the Y_3NbO_7 phase, which is impossible to get in a pure form via the ceramic route even at 1400 °C [15]. Because of the limitations of the solid-state synthesis, alternatives based on metal precursors have been exploited for the Y-based oxides mentioned above, but in a very less extended way than the ceramic route. The main advantage of precursors methods in general is their ability to provide homogeneous and crystalline materials under conditions significantly milder than those employed in conventional solid-state synthesis, and displaying relatively high specific surface areas. Okubo and Kakihana reported the synthesis via a modified polymerizable complex method of the Y_3NbO_7 oxide, which can then be obtained in a pure form at reduced temperatures (500–700 °C) [28]. A pure monoclinic $YNbO_4$ phase with a fergusonite-type structure (described as the M-phase) can also be obtained at 600 °C with a relatively high specific surface area by a citrate method, starting from complexes of yttrium and niobium prepared in situ from the corresponding chlorides and citric acid in alcohol medium [29]. And finally, alkoxide-based methods have also been developed in order to decrease the treatment temperature of the precursor between 600 and 700 °C. These preparation routes have been allowed to reach a metastable tetragonal phase of $YNbO_4$ [30,31]. The temperature-dependent polymorphism of the $YNbO_4$ oxide will be detailed in the discussion.

We present here the development of a novel preparation method for the formation of the $Bi_{1-x}Y_xO_{1.5}$ solid solution, and the Y_3NbO_7 and $YNbO_4$ phases at moderate temperatures. This molecular precursor route is an aqueous way and starts from stable and water-soluble pre-isolated metal precursors that are coordination compounds of yttrium, bismuth and niobium with the ethylenediaminetetraacetate ligand (edta).

2. Experimental section

2.1. Syntheses of precursors

The synthesis of the yttrium(III) precursor, $Y(Hedta)\cdot 2.5H_2O$ was obtained from the following procedure: H_4edta (2 g, 0.0068 mol) was dissolved in 200 mL boiling distilled water. $Y_2(CO_3)_3$ (1.31 g, 0.0034 mol) was slowly added to the clear solution of the ligand and the resulting mixture was refluxed until complete dissolution of the carbonate. The concentration of the solution under reduced pressure up to a final volume of 10 mL yielded a fine white solid which was filtered off and air-dried. *Anal.* Found: C 28.13, H 3.74, N 6.29. Calc. for $C_{10}H_{18}YN_2O_{10.5}$: C 28.36, H 4.25, N 6.62%.

The bismuth(III) compound used (gu)[Bi(edta)(H_2O)] (gu = guandinium, $CN_3H_6^+$) was also obtained according to a reported synthesis [32]: H_4edta (3 g, 0.01 mol) was dissolved in boiling water and bismuth oxocarbonate $(BiO)_2CO_3$ (2.61 g, 0.005 mol) was then added. The obtained suspension was refluxed for 6 h until complete dissolution. $(gu)_2CO_3$ (0.92 g, 0.005 mol) was added and the progressive elimination of solvent under reduced pressure provided a white crystalline solid which was filtered off and air-dried. *Anal.* Found: C 22.78, H 3.48, N 11.88. Calc. for $C_{11}H_{20}BiN_5O_9$: C 22.94, H 3.48, N 12.17%.

The guanidinium (gu) salts of the peroxo-edta precursors of niobium(V) $(gu)_3[Nb(O_2)_2(edtaO_2)]\cdot 2H_2O$ was prepared in aqueous medium by substituting two peroxo groups by the edta ligand in the tetraperoxometallate anion $(gu)_3[Nb(O_2)_4]$, according to a procedure described in details elsewhere [33]. The synthesis was carried out in the presence of excess hydrogen peroxide (35 wt%, Acros) which led to the direct formation of complexes with the bis(N-oxide) derivative of the edta ligand. *Anal.* Found: C 22.36, H 5.02, N 22.03. Calc. for $C_{13}H_{34}N_{11}NbO_{16}$: C 22.50, H 4.90, N 22.21%.

2.2. Oxides preparation

The mixed Y–M (M = Bi or Nb) and Bi-doped Y–Nb oxides were prepared by a method engaging edta complexes as precursors. The detailed preparation scheme is illustrated in Fig. 1. The corresponding precursors were dissolved together and simultaneously in distilled water according to the appropriate metal proportions. The resulting clear solution was then stirred at room temperature for 1 h. The solvent was gently eliminated for 6 h by a freeze-drying process. The resulting mixed solid precursor was pre-calcined at 300 °C for 24 h in flowing air, yielding an amorphous material which was then calcined for 24 h in flowing air. The calcination temperature was varied from 600 to 1000 °C in order to optimize the thermal conditions for the formation of the pure phases of interest.

In the case of the Bi–Y system, in order to reach the $Bi_{1-x}Y_xO_{1.5}$ solid solution in a composition range corresponding to the highest conductivity, several values of x

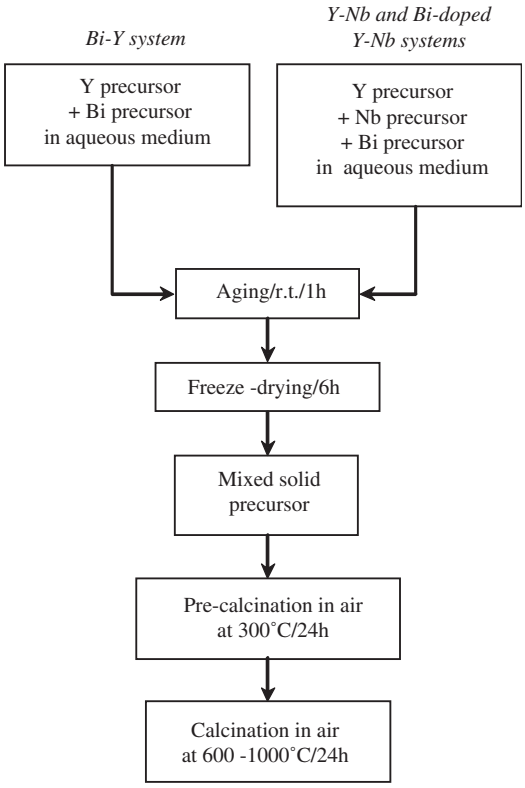

Fig. 1. Preparation scheme of the mixed Bi–Y, Y–Nb and Bi-doped Y–Nb oxides.

were used: 0.22, 0.25 and 0.3. For the Y–Nb system, Y/Nb molar ratios of 3 and 1 were engaged, the first ratio corresponding to the Y_3NbO_7 (namely the $Y_{1-x}Nb_xO_{1.5+x}$ solid solution when $x = 0.25$), and the second one corresponding to the stoichiometric $YNbO_4$ phase. In the case of the Bi-doped Y–Nb samples, the (Y + Bi)/Nb engaged is equal to 1 and the molar percentage in bismuth is either 0.5% or 1% with respect to total Bi + Y amount.

Care should be exercised when heating a peroxo-type precursor like that engaged for niobium. Removal of solvent upon heating in vacuum should be avoided. The successive use of the "soft" freeze-drying process to eliminate the solvent first, followed by a pre-calcination step processed in an oven at a relatively moderate temperature (300 °C), is preferable for security reasons.

2.3. Characterization

Elemental analyses (C, H, N) were carried out at the University College of London. Thermogravimetry (TG) was performed in air at the heating rate of 10 °C min^{-1} using a Mettler Toledo TGA/SDTA851^e analyzer. Powder X-ray diffraction (XRD) was carried out at room temperature on a SIEMENS D-5000 diffractometer using the CuKα radiation ($\lambda = 1.5418$ Å). The samples were placed on quartz monocrystals and the crystalline phases were identified by reference to the JCPDS-ICDD database. FT-Raman spectra were recorded on a Bruker spectrometer (type RFS100/S) at the wavelength of 1064 nm.

3. Results and discussion

3.1. Thermal analyses of the mixed precursors

The mixed solid precursors obtained from the freeze-drying process were analysed by TG before the further calcination step. Examples of thermograms for Bi–Y and Y–Nb mixed precursors obtained after freeze-drying are illustrated in Fig. 2. The TG analyses of the solid Bi–Y mixed precursors show a multi-step decomposition. After the dehydration step around 100 °C, each precursor decomposes into the oxide up to a final temperature which reaches approximately 450 °C, whatever the Y/Bi composition engaged. The TG analyses of the Y–Nb mixed solid precursors display a multi-step decomposition into the oxide, with a final temperature which is the same for both samples characterized by Y/Nb molar ratios of 1 and 3, but which is higher than in the case of the Bi–Y system. This final decomposition temperature reaches 625 °C and is also the same for the Bi-doped Y–Nb precursors as for the corresponding undoped samples.

3.2. Bi–Y oxides

The XRD patterns of the mixed Bi–Y precursor with different metal molar ratios show that these starting materials are all amorphous. When calcining the precursors at 600 °C, the diffractograms display in each case the presence of the $Bi_{1-x}Y_xO_{1.5}$ solid solution in its rhombohedral form (JCPDS file 40-1021), while on further increasing the calcination temperature, the rhombohedral oxide disappears. It is progressively replaced by the $Bi_{1-x}Y_xO_{1.5}$ oxide in its cubic form (JCPDS file 33-0223), which is the most interesting one in term of application in ionic conductivity. This cubic oxide is obtained in a pure form at 650 °C in the case of $x = 0.22$ and 0.25, and at 700 °C when $x = 0.3$. Fig. 3 illustrates the evolution of the diffractograms of the Bi–Y samples with $x = 0.25$, from the stage of the amorphous precursor to the cubic oxide.

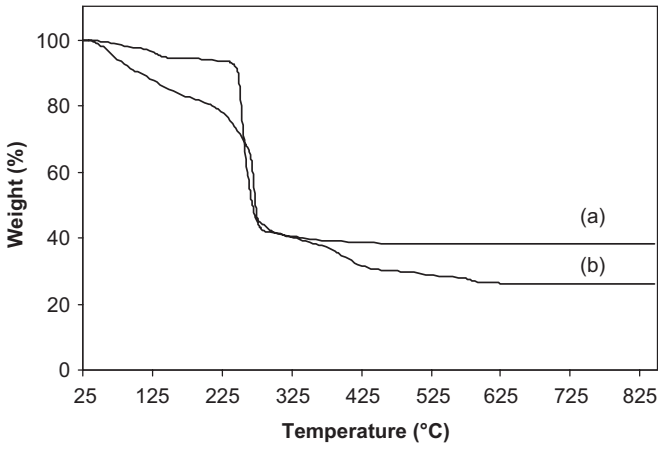

Fig. 2. Thermograms under flowing air of the freeze-dried Bi–Y precursors used for (a) $Bi_{1-x}Y_xO_{1.5}$ ($x = 0.25$) and (b) Y_3NbO_7 oxides.

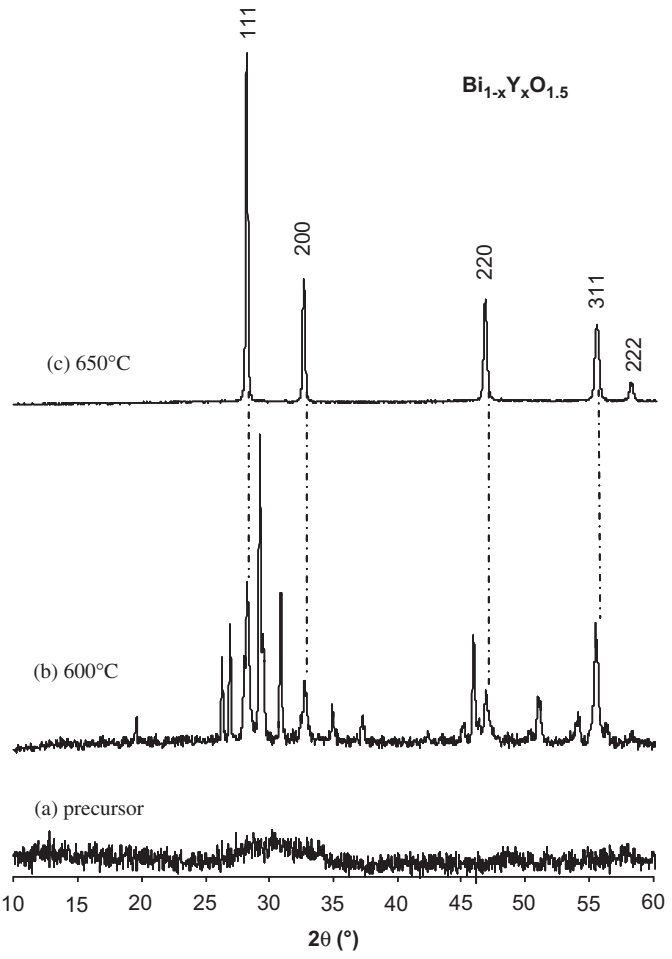

Fig. 3. Diffractograms of the freeze-dried Bi–Y precursors used for the $Bi_{1-x}Y_xO_{1.5}$ oxide ($x = 0.25$) (a), and after calcination at 600 °C (b) and at 650 °C (c). The dashed line indicates the diffraction lines from the cubic phase (JCPDS file 33-0223), the other lines corresponding to the rhombohedral oxide (JCPDS file 40-1021).

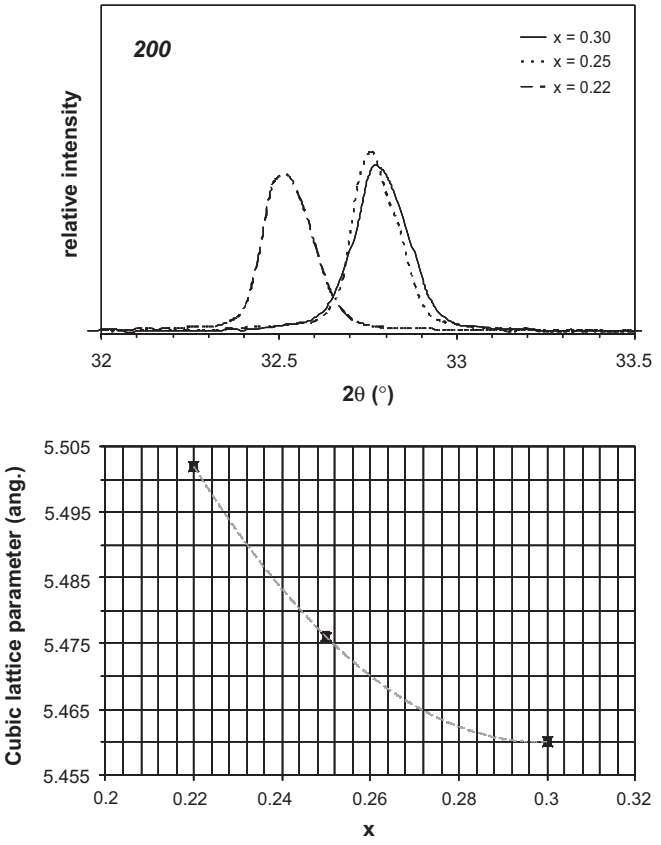

Fig. 4. (a) Evolution of the position of the 200 diffraction line in the diffractograms of the pure cubic $Bi_{1-x}Y_xO_{1.5}$ oxides as a function of the composition, x. The cubic lattice parameter a is plotted as a function of x in (b).

The similarity of the diffractograms obtained for the three x values shows that these materials are isostructural, only slight shifts in 2θ values being observed for most of the diffraction lines occurring from the cubic lattice. These 2θ shifts for the 200 line as well as the evolution of the cubic lattice parameter a (calculated from Bragg's Law) with the composition are illustrated in Fig. 4. When the yttrium content (x) increases, we observe that the lattice parameter decreases regularly. A similar non-linear trend was previously evidenced in the same composition region for the cubic $Bi_{1-x}Y_xO_{1.5}$ solid solution [9].

The Raman analyses of the $Bi_{1-x}Y_xO_{1.5}$ oxides are illustrated in Fig. 5(a) for the three x values. These spectra show only one very broad band which occurs near $625\,cm^{-1}$ and which is actually slightly shifted with the composition. When the Y content increases, the band is significantly displaced to higher wavenumbers, in line with the fact that Bi is heavier than Y (Fig. 5(b)). The Raman bands concerned by this behavior are therefore assumed to correspond to vibrational modes of metal/oxygen bonds influenced by the local environment. A similar but reverse behaviour of Raman bands was previously observed for solid solutions appearing in the Nb_2O_5–Ta_2O_5 system [34]. Another behaviour of the band near $625\,cm^{-1}$ in the spectra of the $Bi_{1-x}Y_xO_{1.5}$ oxides is its variation in relative intensity. As also illustrated in Fig. 5(b), the intensity of the band is linearly related to the x value: it significantly decreases with an increasing Y amount.

3.3. Undoped and Bi-doped Y–Nb oxides

Powder XRD studies at room temperature of the Y–Nb samples revealed those materials to display different compositions, depending on the Y/Nb molar ratio and on the calcination temperature.

In the case of the sample characterized by a Y/Nb molar ratio of 3, the cubic Y_3NbO_7 phase is detected after calcination of the corresponding freeze-dried precursor at 650 °C, as illustrated in Fig. 6(b) (JCPDS file 36-1353). The crystallization process of this phase however begins at the lower temperature of 600 °C (Fig. 6(a)).

In the case of the sample characterized by a Y/Nb molar ratio of 1 and without bismuth doping, the diffractogram at room temperature of the sample obtained after thermal treatment at 750 °C revealed the simultaneous presence of both binary oxides, Y_2O_3 and Nb_2O_5; after heating at

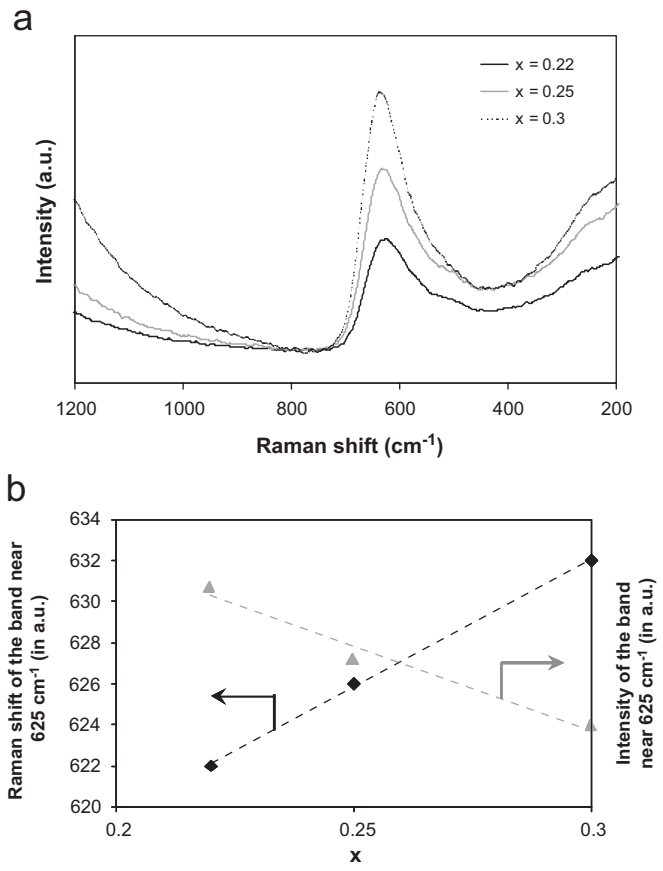

Fig. 5. (a) Raman spectra of the cubic $Bi_{1-x}Y_xO_{1.5}$ oxides as a function of the composition and (b) the evolution of Raman shift and relative intensity of the band near 625 cm^{-1}.

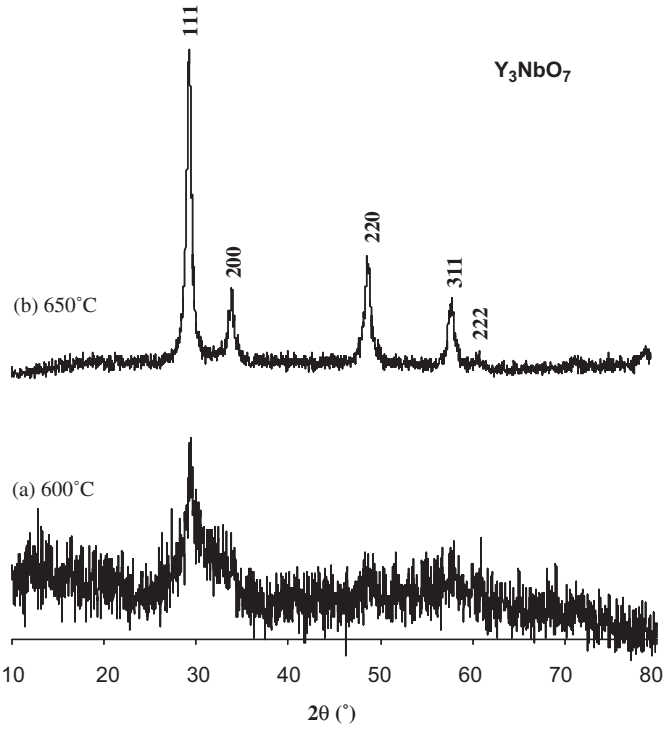

Fig. 6. Diffractograms at r.t. of the mixed Y–Nb precursor (Y/Nb = 3) obtained after calcination (a) at 600 °C and (b) at 650 °C. Indexation is made on the basis of the JCPDS file 36-1353.

800 °C, the XRD pattern displayed the formation of a pure tetragonal $YNbO_4$ phase with a distorted structure (JCPDS file 38-0187, Fig. 7(b)), usually referred to as the T′-form.

According to the literature, the $YNbO_4$ oxide has two main polymorphs: (a) a low-temperature monoclinic form (M-type form) which is the thermodynamically stable one at room temperature, and (b) a high-temperature tetragonal form (T structure), which is unstable and transforms into the monoclinic oxide when cooled to room temperature [12,29–31]. Up to now, only the monoclinic form of $YNbO_4$ has been preserved at room temperature when prepared by a ceramic route [12,14,18,26,29,35], whereas the T-phase has never been observed at room temperature. A distorted form of the tetragonal phase, designated as the T′-phase, also exists and it has been obtained by soft chemical methods, either by starting from an amorphous mixed precursor prepared by the simultaneous hydrolysis of Y and Nb alkoxides followed by a quenching of the phase heated at 750 °C [31], or by a sol–gel method followed by calcination of the gel near 600 °C [30].

In the present work, the molecular precursor method used also allows forming the distorted tetragonal T′-form of $YNbO_4$ by calcination at 800 °C and stabilizing it at room temperature. However, the broad diffraction lines observed for that phase (Fig. 7(b)) can be interpreted by the presence of small amounts of the monoclinic M-phase (see Fig. 7(a)). The significant broadening of the lines in XRD was previously pointed out for this phase by Yamagushi et al. and it was explained by a large

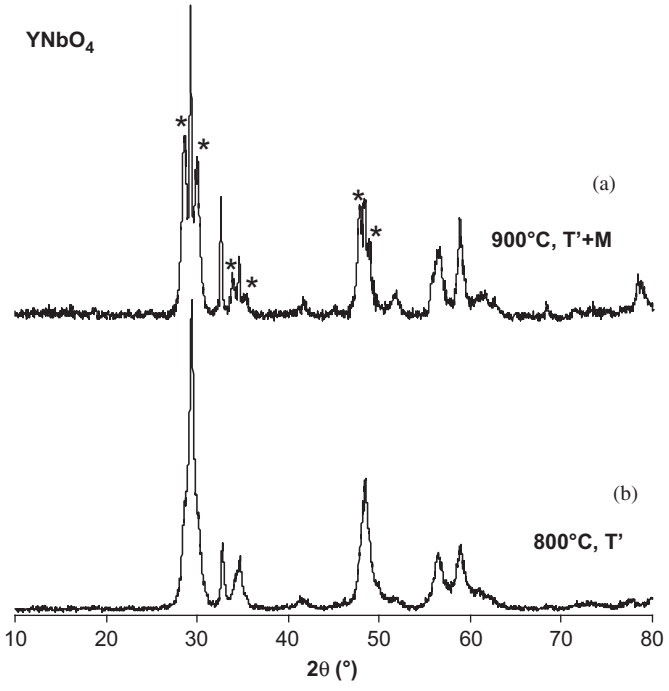

Fig. 7. Evolution of the diffractograms at r.t. of the $YNbO_4$ samples with the calcination temperature. The * signs indicate the major diffraction lines occurring from the monoclinic $YNbO_4$ (JCPDS file 23-1486), the other ones come from the T′ structure.

fluctuation of the interplanar spacing in the distorted structure [31].

When heat-treating the mixed precursor with Y/Nb = 1 at temperatures higher than 800 °C, diffraction lines from the monoclinic $YNbO_4$ phase (JCPDS file 23-1486) begin to appear clearly (850 and 900 °C) and the latter becomes the major phase when calcining up to 1100 °C. This phases evolution upon heating, illustrated in Fig. 7, is due to a T′ to T transformation, which occurs between 820 and 880 °C according to Yamagushi et al. [31]. Upon cooling down to room temperature, the unstable high-temperature T-form obtained in this work near 850–900 °C converts into the thermodynamically stable M-phase. This behaviour of the $YNbO_4$ oxide, which was previously observed by Mather and Davies when using a sol–gel method but at lower temperatures, is schematized in Scheme 1(a) [30].

When doping the $YNbO_4$ oxide with small amounts of Bi^{3+} (0.5% and 1% Bi with respect to total Bi + Y amount), the diffractograms of the samples heated at 800 °C showed, in addition to lines from the tetragonal T′ structure, other lines characteristic of the monoclinic form of $YNbO_4$. Fig. 8 provides a comparison between the undoped $YNbO_4$ oxide with a distorted tetragonal T′ structure and the Bi-doped $YNbO_4$ samples, corresponding to the $Bi_xY_{1-x}NbO_4$ general formula, showing a mixture of both T′- and M-forms. The presence of bismuth thus disturbs the stabilization of the distorted tetragonal T′ structure at room temperature, and leads to the come back of the thermodynamically stable monoclinic form. On the contrary, previous results by Bahng et al. showed that the addition of small amounts of bismuth in the monoclinic $YNbO_4$ phase did not affect the lattice structure and crystallinity of the oxides, but in their work, they only observed the monoclinic form, even for the undoped $YNbO_4$ sample [26]. Moreover, with the precursor method used in the present work, as observed for the undoped oxide, the T′-form disappears when increasing the temperature in profit of the M-form, which is practically pure in that case at 900 °C, whatever the bismuth content. The temperature dependence of the Bi-doped $YNbO_4$ oxide is illustrated in Scheme 1(b), considering the monoclinic M-phase experimentally observed to be derived from the unstable T′ oxide upon cooling to room temperature.

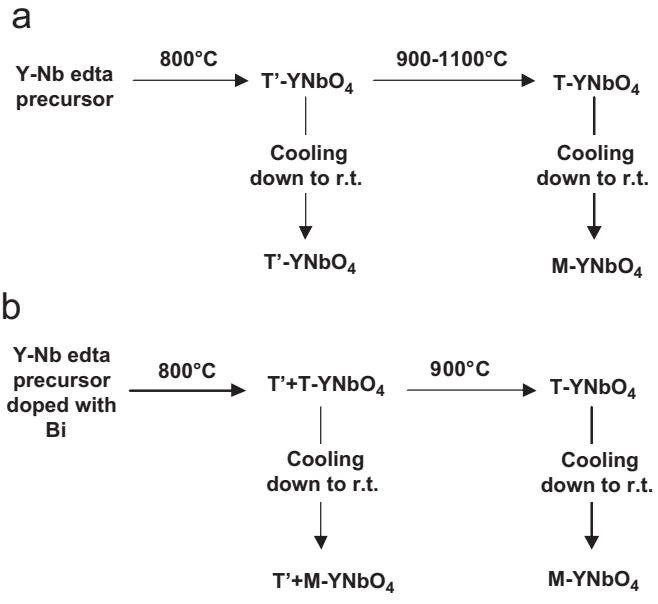

Scheme 1. Temperature-dependent polymorphism of undoped (a) and bismuth-doped (b) $YNbO_4$ obtained from the calcination of a mixed edta-type precursor.

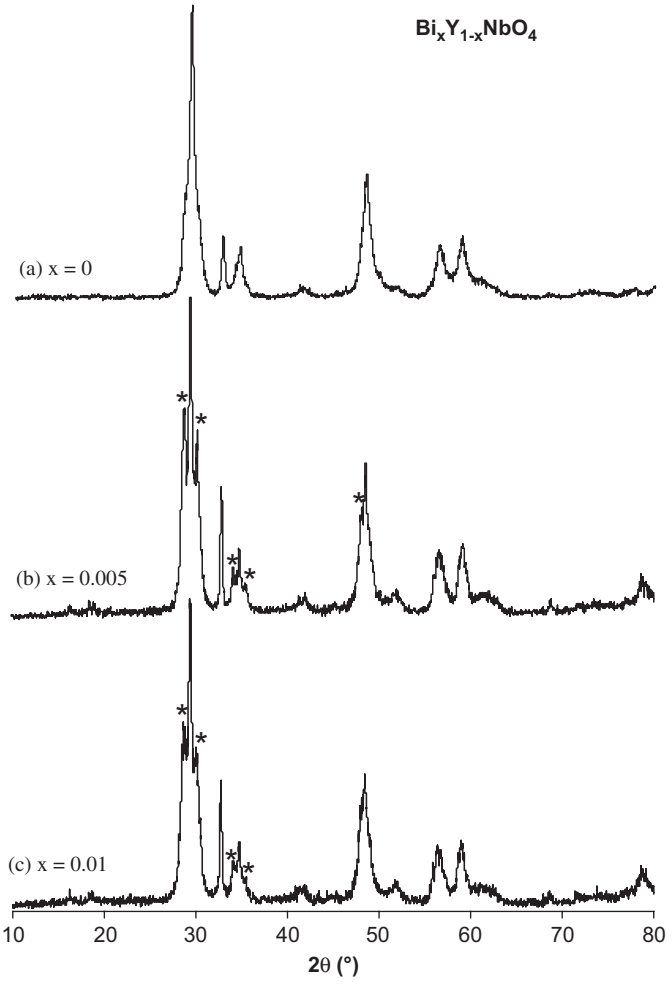

Fig. 8. Diffractograms at r.t. of the $Bi_xY_{1-x}NbO_4$ samples obtained after calcination at 800 °C, with $x = 0$ (undoped oxide) (a), 0.005 (b) and 0.01 (c). The diffractograms in (a) corresponds to the T′-phase of $YNbO_4$ (JCPDS file 38-0187). The * signs in (b) and (c) indicate the major diffraction lines occurring from the monoclinic $YNbO_4$ (JCPDS file 23-1486), the other ones come from the T′ structure.

Raman spectroscopy for the Y–Nb sample with Y/Nb = 3 confirmed the XRD results and is in agreement with an identical analysis reported previously for the Y_3NbO_7 phase [35]. The Raman spectrum displays broad bands centered at 774, 348 and 167 cm^{-1}. The positions of these bands are compared in Table 1 with the values previously reported by Yashima et al. [35]. Some differences can be evidenced between the two sets of data, but this can be explained by the width and the weak intensity of

Table 1
Raman shifts (in cm^{-1}) observed for the cubic Y_3NbO_7 and tetragonal T′-$YNbO_4$ pure oxides obtained at 650 and 800 °C, respectively. The experimental values are compared with Raman and IR data from the literature [30,34]

	Raman data		IR data	
	This work (cm^{-1})	Ref. [34] (cm^{-1})	Ref. [30] (cm^{-1})	
Y_3NbO_7	788	778	–	–
	348	392	–	–
	–	244	–	–
	167	130	–	–
	T′-phase	M-phase	T′-phase	M-phase
$YNbO_4$	811	811	810	810
	695	688	700	705
	679	675		
	661	658	645	640
	–	–	600	600
	–	–	555	550
	465	465	460	475
	441	439	–	–
	423	428	–	–
	341	336	–	–
	328	324	–	–
	238	233	–	–
	215	213	–	–
	166	161	–	–
	136	131	–	–

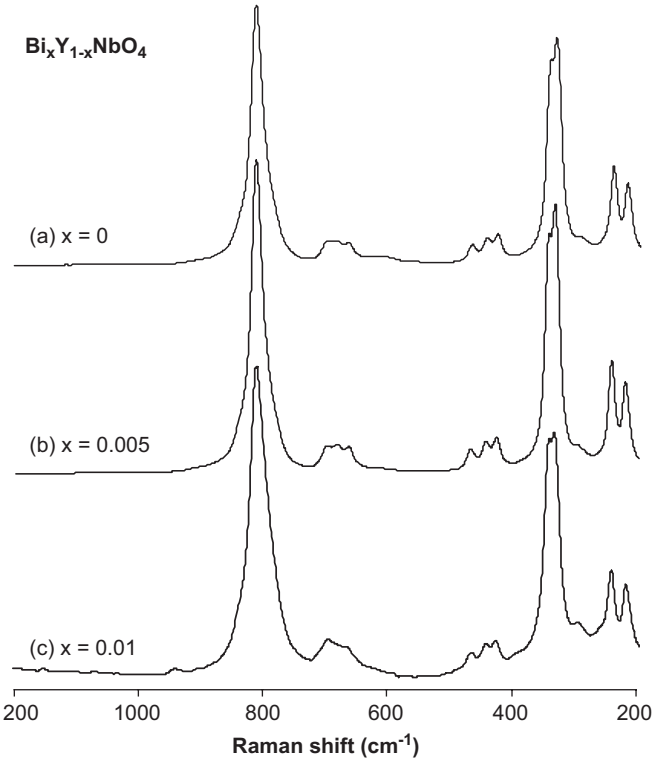

Fig. 9. Raman spectra of the $Bi_xY_{1-x}NbO_4$ samples obtained after calcination at 800 °C, with $x = 0$ (undoped oxide) (a), 0.005 (b) and 0.01 (c).

most Raman lines. The sample with a Y/Nb = 1 gives rise to an intense Raman response (Fig. 9(a)) and the spectrum contains a lot of sharp bands which are also listed in Table 1. The Raman spectrum of the pure T′-$YNbO_4$ phase, first observed in this work by XRD, totally matches the analysis previously reported for the monoclinic M-$YNbO_4$ [35], as illustrated in the comparison given in Table 1. Both T′- and M-phases thus present the same vibrational spectral pattern. This is in agreement with the observation of Yamagushi et al. who evidenced similar infrared data for these two phases (Table 1) and who concluded that the T′- and M-phases are characterized by the same moeities, namely tetrahedral NbO_4 groups [31]. According to Petrov et al., the band near 800 cm^{-1} is due to the symmetrical stretching of these groups, $\nu_s(NbO_4)$ and the bands in the 750–500 cm^{-1} range are due to their antisymmetrical stretching vibrations, $\nu_{as}(NbO_4)$. One or two bands due to the Y–O stretching mode are located in the 480–400 cm^{-1} region [36]. In the case of the bismuth doping of the $YNbO_4$ phase, we observed by XRD the formation of a mixture of the tetragonal T′- and monoclinic M-forms (Fig. 8). This mixture cannot be detected by Raman spectroscopy because, as we just described above, both phases are not discernible by this technique. The Raman spectra of the $Bi_xY_{1-x}NbO_4$ samples with $x = 0.005$ and 0.01 are all exactly the same and identical to that obtained for the tetragonal $YNbO_4$ (Fig. 9). Moreover, no variation of Raman shift is observed between the undoped and doped samples.

4. Conclusions

A molecular precursor route based on stable, stoichiometrically well-defined and water-soluble pre-isolated edta complexes has been developed and applied to the preparation of a series of yttrium-containing mixed oxides which are known for their attractive properties in domains like ionic conductivity and luminescence.

The cubic $Bi_{1-x}Y_xO_{1.5}$ solid solution (with $x = 0.22$, 0.25 and 0.3) and Y_3NbO_7 oxide have been obtained in a pure form in a range of moderate temperatures (600–650 °C), in comparison with the commonly used ceramic method which requires temperatures reaching sometimes 1500 °C. This preparation method has also allowed to stabilize at room temperature, without quenching, the tetragonal $YNbO_4$ oxide in a distorted form (T′-phase) by calcining the precursor at 800 °C. When heating further, this metastable T′-phase transforms into the T oxide, which converts on cooling down to room temperature into the more stable monoclinic M oxide (1100 °C). Doping the $YNbO_4$ oxide with bismuth has led, after heating at 800 °C, to a mixture of the distorted tetragonal T′ and the thermodynamically stable monoclinic phase. After thermal treatment at 900 °C, the practically pure monoclinic structure has been obtained upon cooling down to room temperature.

Even if the general behaviour of the phases existing in the studied Bi–Y and Y–Nb systems is already known, the preparation method taken into account to obtain them has

a drastic influence on the structure of the resulting oxides. We have seen in this work that the nature of the phases observed as well as the temperatures required to reach them is very different from other routes developed previously, namely the solid-state ceramic method, alk-oxide-based routes or even an aqueous polymeric resin approach.

The main advantages of the precursors method described in this work in general are (i) its ability to reach the pure desired phases at relatively moderate temperatures and (ii) its ability to stabilize at room temperature metastable oxide structures, which are often inaccessible via a solid-state way. We could also point out that (iii) complexes with the edta ligand are known for a lot of transition metals and generally easy to synthesize and stable towards moisture, which is important as far as particular metals, like niobium, are concerned, and, finally (iv) water constitutes an environment friendly medium for syntheses.

Acknowledgments

The authors thank the Belgian National Fund for Scientific Research (FNRS) for the Research fellowship allotted to D.A. Bayot and financial support. They also thank CBMM company (Brazil) and Niobium Products Company GmbH (Germany) for supplying niobic acid and financial support.

References

[1] T. Takahashi, H. Iwahara, T. Arao, J. Appl. Electrochem. 10 (1980) 677.
[2] E.M. Levin, R.S. Roth, J. Res. Natl. Bur. Stand. A 68 (1964) 189.
[3] H. Iwahara, T. Esaka, T. Sato, J. Solid State Chem. 39 (1981) 173.
[4] M.J. Verkerk, A.J. Burggraaf, Solid State Ion. 3–4 (1981) 463.
[5] T. Takahashi, H. Iwahara, Mater. Res. Bull. 13 (1978) 1447.
[6] A. Watanabe, T. Kukuchi, Solid State Ion. 21 (1986) 287.
[7] P.D. Battle, C.R.A. Catlow, A.V. Chadwick, P. Cox, G.N. Greaves, L.M. Moroney, J. Solid State Chem. 69 (1987) 230.
[8] P.D. Battle, B. Montez, E. Oldfield, J. Chem. Soc. Chem. Commun. (1988) 584.
[9] R.K. Datta, J.P. Meehan, Z. Anorg. Allg. Chem. 383 (1971) 328.
[10] W.W. Barker, J. Mater. Sci. Lett. 3 (1984) 492.
[11] H. Kobayashi, H. Ogino, T. Mori, H. Yamamura, T. Mitamura, J. Ceram. Soc. Jpn. Int. Ed. 101 (1993) 654.
[12] J.H. Lee, M. Yashima, M. Kakihana, M. Yoshimura, J. Am. Ceram. Soc. 81 (1998) 894.
[13] H.P. Rooksby, E.A.D. White, J. Am. Ceram. Soc. 47 (1964) 94.
[14] T. Ishihara, K. Sato, Y. Mizuhara, Y. Takita, Solid State Ion 50 (1992) 227.
[15] H. Kobayashi, H. Kuramochi, H. Ogino, T. Mori, H. Yamamura, T. Mitamura, J. Ceram. Soc. Jpn. 100 (1992) 960.
[16] Y.J. Sun, H.J. Liu, X. Wang, X.G. Kong, H. Zhang, Chem. Mater. 18 (2006) 2726.
[17] A.K. Levine, F.C. Palilla, Appl. Phys. Lett. 5 (1964) 118.
[18] A.H. Buth, G. Blasse, Phys. Status Solidi A—Appl. Res. 64 (1981) 669.
[19] S.K. Lee, H. Chang, C.H. Han, H.J. Kim, H.G. Jang, H.D. Park, J. Solid State Chem. 156 (2001) 267.
[20] G. Blasse, A. Bril, J. Lumin. 3 (1970) 109.
[21] S.L. Issler, C.C. Torardi, J. Alloy Compd. 229 (1995) 54.
[22] L.I. Kazakova, A.B. Dubovsky, G.V. Semenkovich, O.A. Ivanova, Radiat. Meas. 24 (1995) 359.
[23] L.I. Kazakova, I.S. Bykov, A.B. Dubovsky, J. Lumin. 72–74 (1997) 211.
[24] W.J. Schipper, M.F. Hoogendorp, G. Blasse, J. Alloy Compd. 202 (1993) 283.
[25] G. Panayiotakis, D. Cavouras, I. Kandarakis, C. Nomicos, Appl. Phys. A—Mater. Sci. Process. 62 (1996) 483.
[26] J.H. Bahng, E.S. Oh, S.H. Seo, J.S. Kim, M. Lee, H.L. Park, C.I. Lee, G.C. Kim, K.J. Kim, Phys. Status Solidi A—Appl. Res. 191 (2002) 291.
[27] S.H. Shin, D.Y. Jeon, K.S. Suh, J. Appl. Phys. 90 (2001) 5986.
[28] T. Okubo, M. Kakihana, J. Alloy Compd. 256 (1997) 151.
[29] C. Quinn, R. Wusirika, J. Am. Ceram. Soc. 74 (1991) 431.
[30] S.A. Mather, P.K. Davies, J. Am. Ceram. Soc. 78 (1995) 2737.
[31] O. Yamagushi, K. Matsui, T. Kawabe, K. Shimizu, J. Am. Ceram. Soc. 68 (1985) C275.
[32] A.B. Ilyukhin, R.L. Davidovich, V.B. Logvinova, H.K. Fun, S.S.S. Raj, I.A. Razak, S.Z. Hu, S.W. Ng, Main Group Met. Chem. 22 (1999) 275.
[33] D. Bayot, B. Tinant, M. Devillers, Catal. Today 78 (2003) 439.
[34] D.A. Bayot, M.M. Devillers, Chem. Mater. 16 (2004) 5401.
[35] M. Yashima, J.-H. Lee, M. Kakihana, M. Yoshimura, J. Phys. Chem. Solids 58 (1997) 1593.
[36] K.I. Petrov, N.V. Gundobin, V.V. Kravchenko, S.S. Plotkin, Zh. Neorg. Khim. 18 (1973) 928.